Electro-Osmotic Flow in Micro-Channels With Finite Inertial and Pressure Forces

ARTICLE *in* ANALYTICAL CHEMISTRY · JUNE 2001

Impact Factor: 5.64 · DOI: 10.1021/ac0101398 · Source: PubMed

1 AUTHOR:

Juan G Santiago
Stanford University
307 PUBLICATIONS **10,516** CITATIONS

SEE PROFILE

Anal. Chem. **2001,** *73,* 2353−2365

Electroosmotic Flows in Microchannels with Finite Inertial and Pressure Forces

J. G. Santiago

Department of Mechanical Engineering, Stanford University, Stanford, California 94305

Emerging microfluidic systems have spurred an interest in the study of electrokinetic flow phenomena in complex geometries and a variety of flow conditions. This paper presents an analysis of the effects of fluid inertia and pressure on the velocity and vorticity field of electroosmotic flows. In typical on-chip electrokinetics applications, the flow field can be separated into an inner flow region dominated by viscous and electrostatic forces and an outer flow region dominated by inertial and pressure forces. These two regions are separated by a slip velocity condition determined by the Helmholtz−Smoulochowski equation. The validity of this assumption is investigated by analyzing the velocity field in a pressure-driven, two-dimensional flow channel with an impulsively started electric field. The regime for which the inner/outer flow model is valid is described in terms of nondimensional parameters derived from this example problem. Next, the inertial forces, surface conditions, and pressure-gradient conditions for a full-field similarity between the electric and velocity fields in electroosmotic flows are discussed. A sufficient set of conditions for this similarity to hold in arbitrarily shaped, insulating wall microchannels is the following: uniform surface charge, low Reynolds number, low Reynolds and Strouhal number product, uniform fluid properties, and zero pressure differences between inlets and outlets. Last, simple relations describing the generation of vorticity in electroosmotic flow are derived using a wall-local, streamline coordinate system.

Electroosmosis describes the motion of fluids with respect to a fixed, charged solid surface. This flow results when an electric field is applied to the electrical double layer that spontaneously forms at the interface between a liquid and solid when they are brought into contact.[1] The thickness of this double layer is determined by the opposing forces of electrostatic attraction and thermal diffusion and is on the order of the Debye length of the solution. The advent of microfluidic fabrication technologies has seen an application of electroosmosis as a method of controlling fluids in microfluidic chips.[2,3] On-chip electroosmotic pumping is readily incorporated into electrophoretic and chromatographic separations, and these "laboratories on a chip" offer distinct advantages over the traditional, free-standing capillary systems including the ability to network multiple channel streams and reduce analysis time.

Various studies dealing with electroosmotic flow theory and modeling have analyzed the effects of flow inertia, pressure gradients, and nonuniform ζ-potentials in microfluidic channels. Anderson and Idol[4] analyzed electroosmotic flow in channels with nonuniform surface charge. Anderson[5] presented an analysis that shows electrical double layers reach a local equilibrium in the presence of electroosmosis when the channel length is long compared to the characteristic hydraulic diameter. Dose and Guiochon[6] and Sodermann and Jonsson[7] presented an analysis of the time scales of transient electroosmotic flows. Dose and Guiochon[6] presented a numerical simulation of impulsively started electroosmotic flow, while Sodermann and Jonsson presented analytical models for start-up electroosmotic flows in a variety of flow geometries including flow over a single flat plate and flow between two flat plates. More recently, Patankar and Hu[8] developed a numerical model for electroosmotic flow in a microchannel network and used this numerical model to demonstrate an apparent Reynolds number dependence of electroosmotic flow through a microchannel intersection. Other electroosmotic flow numerical simulations include those of Ermakov et al.[9] and Bianchi et al.[10]

In the simplest case, internal electroosmotic flows in arbitrary geometries are well approximated by simple irrotational flow models.[11] This idea was first proposed by Overbeek,[12] who considered low Reynolds number, steady electroosmotic flow in microchannels with arbitrary geometry, and zero pressure gradient. Overbeek showed that, for channels with relatively thin charge layers, the flow field outside of the double layer is an irrotational flow with a slip velocity condition determined by the Helmholtz−Smoulochowski equation. This simplification has also been shown by Morrison[13] for the electrophoretic flow around a charged

(1) Bockris, J.; Reddy, A. *Modern Electrochemistry 1: Ionics*, 2nd ed.; Plenum Press: New York, 1998.
(2) Jacobson, S. C.; Hergenroder, R.; Koutny, L. B.; Ramsey, J. M. *Anal. Chem.* **1994**, *66*, 1114−1118.
(3) Manz, A.; Effenhauser, C. S.; Burggraf, N.; Harrison, D. J.; Seiler, K.; Fluri, K. *J. Micromechan. Microeng.* **1994**, *4*, 257−265.
(4) Anderson, J. L.; Idol, W. K. *Chem. Eng. Commun.* **1985**, *38*, 93−106.
(5) Anderson, J. L. *J. Colloid Interface Sci.* **1985**, *105*, 45−54.
(6) Dose, E. V.; Guiochon, G. *J. Chromatogr.* **1993**, *652*, 263−275.
(7) Soderman, O.; Jonsson, B. *J. Chem. Phys.* **1996**, *105*, 10300−10311.
(8) Patankar, N. A.; Hu, H. H. *Anal. Chem.* **1998**, *70*, 1870−1881.
(9) Ermakov, S. V.; Jacobson, S. C.; Ramsey, J. M. *Anal. Chem.* **1998**, *70*, 4494−4503.
(10) Bianchi, F.; Ferrigno, R.; Girault, H. H. *Anal. Chem.* **2000**, *72*, 1987−1993.
(11) Rahman, M. *Potential Flow of Fluids*; WIT Press: Southampton, U.K., 1995.
(12) Overbeek, J. T. G. In *Colloid Science*; Kruyt, H. R., Ed.; Elsevier: Amsterdam, 1952; Vol. 1.
(13) Morrison, F. A. *J. Colloid Interface Sci.* **1970**, *34*, 210−214.

10.1021/ac0101398 CCC: $20.00
Published on Web 04/12/2001

sphere with a thin double layer. Recently, Cummings et al.[14] proposed an analytical formulation which argues that the similarity between flow velocity and electric field is independent of the effects of fluid inertia. This conclusion is not valid for unsteady flows and may not be true for large Reynolds number flows. The numerical analysis of Patankar and Hu[8] suggests that electroosmotic flows have a Reynolds number dependence, with a significant loss in the fluid velocity/electric field similarity at Reynolds numbers greater than approximately unity.

The current paper presents an analysis of the effects of inertial forces, pressure forces, and nonuniform wall charge on the applicability of a slip velocity approximation and on the vorticity field outside of the electrical double layer. A set of sufficient conditions for a full-field similarity between the electric and velocity fields in electroosmotic flows are also discussed.

FORMULATION OF PROBLEM

Formulations of the equations of motion for electrokinetic flows are given by Probstein[15] for electroosmotic flow through arbitrarily shaped capillary structures and Russel et al.[16] for the electrophoretic flow induced around a charged body. Here, the equations of motion of electroosmotic flow of an incompressible Newtonian fluid will be normalized as follows:

$$\bar{x}' = \bar{x}/d$$

$$t' = t/t^*$$

$$\bar{V}' = \bar{V}/U$$

$$p' = pd/(\eta U)$$

$$\bar{E}' = \bar{E}/E^*$$

$$\rho_E{}' = \rho_E d/(E^*\epsilon) \tag{1}$$

where $\bar{x}$, $\bar{V}$, p, $\bar{E}$, and ρ_E are the position vector, velocity vector field, pressure, electric vector field, and charge density, respectively. These quantities are nondimensionalized using d, U, t^*, E^*, ϵ, and η, which are a microchannel hydraulic diameter, a characteristic electroosmotic flow velocity, a characteristic time scale (e.g., for an applied forcing function), a characteristic electric field, an electrical permittivity of the medium, and a dynamic viscosity, respectively. The equations of motion are then

$$\nabla\cdot\bar{V}' = 0 \tag{2}$$

$$StRe\frac{\partial\bar{V}'}{\partial t'} + Re\bar{V}'\cdot\nabla'\bar{V}' = -\nabla' p' + Re(\epsilon E^{*2}/\rho U^2)\rho_E{}' E' + (\nabla'^2\bar{V}') \tag{3}$$

where the Laplacian and gradient operators are normalized using d. St and Re are the Strouhal and Reynolds numbers, respectively, and defined as

$$Re = \rho U d/\eta \tag{4}$$

$$St = d/t^* U \tag{5}$$

The full Navier−Stokes and Lorentz force formulation given here may be important in some cases as the Reynolds number of electroosmotic flow fields can exceed unity for high-field electrophoresis applications in microchannels. For example, for a fused-silica surface with a −100 mV ζ-potential, a 2 kV/cm applied potential (applicable to on-chip capillary electrophoresis applications[17]) can achieve a flow velocity of order 10 mm/s. For a hydraulic channel diameter of order 100 μm, the Re based on hydraulic diameter for this electroosmotic flow is of order unity.

The components of the time-dependent, nondimensional velocity vector field can be expressed in terms of unit normals as

$$\bar{V}' = u'\hat{x} + v'\hat{y} + w'\hat{z} \tag{6}$$

and the position vector components are x, y, and z. The body force term on the right-hand side of eq 3 is the Lorentz force imparted on the fluid by the local electric field. Through this term, the equations of motion are coupled with the governing equation for the electric field, which is given by Gauss's law as

$$\nabla'\cdot\bar{E}' = -\nabla'^2\phi' = \rho_E{}' \tag{7}$$

where ϕ' is the electric potential nondimensionalized by E^*d. The charge density ρ_E is related to the concentrations of N species of valence z_i as

$$\rho_E = F\sum_{i=1}^{N} z_i c_i \tag{8}$$

where F is Faraday's constant and c_i is the molar concentration of species i. A full formulation of the coupled system of equations includes the convective diffusion equations for each of the charged species in the system.[15,16] The equation for the diffusion of the ith species in a dilute solution is

$$StPe\frac{\partial c_i'}{\partial t'} + Pe\bar{V}'\cdot\nabla' c_i' = \frac{\mathrm{d}E^* z_i F}{RT}\nabla'\cdot(c_i'\nabla'\phi') + (\nabla'^2 c_i') \tag{9}$$

where R is the universal gas constant, T is temperature, and the Pe is the Peclet number defined as

$$Pe = Ud/D \tag{10}$$

and D is the mass diffusion coefficient. The ion concentration can be nondimensionalized by the ion concentration far from the charged wall so that

(14) Cummings, E. B.; Griffiths, S. K.; Nilson, R. H.; Paul, P. H. *Anal. Chem.* **2000**, *72*, 2526−2532.

(15) Probstein, R. F. *Physicochemical Hydrodynamics: An Introduction*, 2nd ed.; John Wiley & Sons: New York, 1994.

(16) Russel, W. B.; Saville, D. A.; Schowalter, W. R. *Colloidal Dispersions*; Cambridge University Press: New.York, 1999.

(17) Fluri, K.; Fitzpatrick, G.; Chiem, N.; Harrison, D. J. *Anal. Chem.* **1996**, *68*, 4285−4290.

$$c_i' = c_i/c_{\infty,i} \tag{11}$$

The first term on the left-hand side of eq 9 describes the local rate of change of the species concentration due to unsteady effects, and the second term describes the local change in concentration due to advection. The two terms on the right-hand side describe the transport of the species due to electromigration and diffusion, respectively. In this formulation, the Nernst−Einstein equation[15] has been used to eliminate the mobility of the ion. The next section uses this formulation to analyze the regime for which a slip velocity approximation is useful in modeling electroosmotic flows.

INNER FLOW AND SLIP VELOCITY APPROXIMATION FOR ELECTROKINETICS

The systems of interest here are microfabricated electroosmotic flow channels and channel networks with characteristic dimensions of order 100 μm. For typical chemical buffer concentrations of order 10 mM, the thickness of the electrical double layer, λ_D, is on the order of a few nanometers.[18] The nondimensionalized double-layer thickness of the channel, λ_D/d is therefore less than 10^{-4} in most bioanalytical applications. Figure 1 shows a schematic of the ion distribution and velocity field associated with the diffuse portion of the electrical double layer and nearby fluid external to the double layer. The region of net charge density and high viscous stress near the wall will here be referred to as the inner flow region of the velocity field, and the velocity field further from the wall will be called the outer flow region. As shown in the figure, the coordinate system for the inner flow region discussed in this section is assumed to be oriented with x (and the x-component of the electric field) in the flow direction and y in the wall-normal direction. The z-velocity component and the spanwise (z) and transverse (y) electric field in this coordinate system can be neglected as can all spanwise gradients.

Diffusion and Electromigration in the Inner Flow Region. A simple order of magnitude scaling argument for the dynamics of the electrical double layer will be presented here while a more detailed analysis of the convective diffusion of ions and charge relaxation is given by Chang et al.[19] The nondimensional parameters in eq 9 reflect the relative importance of transient velocities, advection of charges, electromigration, and diffusion of charges in the electrical double layer. The Peclet number of a typical microchip electroosmotic flow with a $U = 1$ mm/s velocity in a 100-μm channel is on the order of 100 (assuming a diffusivity equivalent to that of a sodium ion). The smallest time scales of interest in electroosmotic flow systems are approximately 1 ms. Such a time scale is much smaller than the ramp times of typical voltage switching schemes. Therefore, the typical values of *Pe* and *StPe* are less than order 10^2 and 10^4, respectively. In comparison, the electromigration term in eq 9 scales as the local electric field in the inner flow region of the electric double layer. The electric field in this region within about a Debye length from the wall is on the order of 10^7 V/m, so the electromigration term is of order 10^6. This electric field is also much larger than (and orthogonal to) the highest applied electric fields in these flows (order 10^5 V/m). Therefore, in estimating the charge distribution of the inner flow region of the electroosmotic flow, we shall ignore the terms on the left-hand side of eq 9 and approximate the charge equilibrium using

$$0 \cong \frac{dE^* z_i F}{RT}\nabla'\cdot(c_i'\nabla'\phi') + (\nabla'^2\, c_i') \tag{12}$$

where we now use the variable ϕ' for the local potential associated with the charges on the wall. This potential is also nondimensionalized by E^*d. Note that the simplification represented by eq 12 is independent of whether d or λ_D are used for the characteristic dimension in the Peclet number since only the ratios of *Pe* to $dE^*z_iF/(RT)$ and *StPe* to $dE^*z_iF/(RT)$ are important. This observation should also hold throughout most of the double layer since any advection-induced charge separation across a dimension on the order of λ_D results in large electric fields which are then rapidly eliminated by electromigration. Another way of justifying this conclusion is to point out that, within the double layer, the time scale associated with electromigration is much shorter than the advective time of the flow.[19]

Equation 12 estimates the equilibrium distribution of ions of species i. For an electrical double layer near a flat wall, the ion density profile is then a Boltzmann distribution of the form

$$\frac{c_i}{c_{\infty,i}} = \exp\left(-\frac{z_i e(y - y_w)\phi}{kT}\right) \tag{13}$$

Here $c_{\infty,i}$ is the molar concentration of ion i in the bulk liquid (far from the wall), z_i is the valance number of the ion, y is a coordinate perpendicular to the wall, y_w is the coordinate of the shear plane, T is temperature, e is the charge of an electron, and k is Boltzmann's constant. The ζ-potential, ζ, is defined as the electric potential at the shear plane of the electrical double layer ($y = y_w$), which is the no slip boundary. For a symmetric electrolyte, eqs 7, 8, and 13 are combined to yield the Poisson−Boltzmann relation:

$$\frac{d^2\phi'}{dy'^2} = \frac{2Fz_ic_\infty d}{\epsilon E^*}\sinh\left(\frac{z_ie(y - y_w)\phi}{kT}\right) \tag{14}$$

Here c_∞ is the molar concentration of each of the two ion species in the bulk. A simplification of this equation, known as the Debye−Hückel approximation,[15] is to consider the case where the argument in the hyperbolic sine function above is small so that

$$\frac{d^2\phi'}{dy'^2} = \left(\frac{d^2}{\lambda_D^{\,2}}\right)\phi' \tag{15}$$

where λ_D is the Debye length of the solution which, for a symmetric electrolyte is simply

$$\lambda_D = \left(\frac{\epsilon kT}{2z^2eFc_\infty}\right)^{0.5} \tag{16}$$

(18) Hiemenz, P. C.; Rajagopalan, R. *Principles of Colloid and Surface Chemistry*; 3rd ed.; Marcel Dekker: New York, 1997.

(19) Chang, J. S.; Kelly, A. J.; Crowley, J. M. *Handbook of Electrostatic Processes*; Marcel Dekker: New York, 1995.

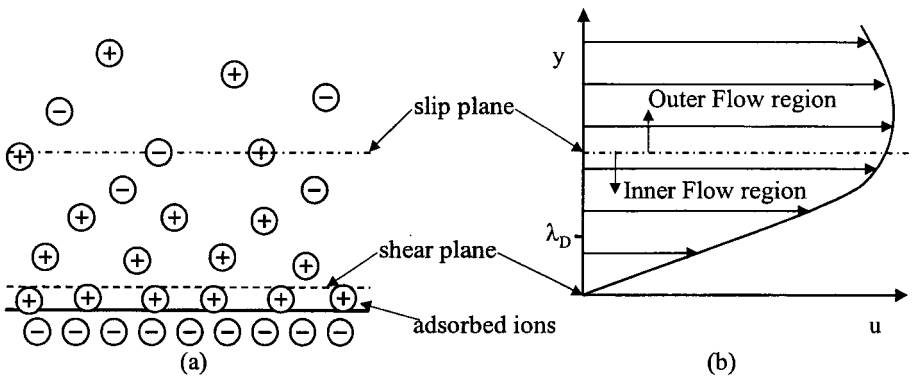

Figure 1. Schematic of the ion distribution and velocity field of the electrical double layer. (a) Diffuse counterions from the bulk electrolyte shield the effective charge density of the shear plane that separates the regions of adsorbed and diffuse ions. (b) The velocity field of the inner and outer regions of the flow separated by a slip plane.

Hunter[20] gave a general solution for eq 14 which can be expressed as

$$\exp\left(\frac{\tilde{\phi}}{2}\right) = \frac{a + b\exp[-(y - y_w)/\lambda_D]}{a - b\exp[-(y - y_w)/\lambda_D]} \tag{17}$$

where

$$a \equiv \exp\left(\frac{\tilde{\zeta}}{2}\right) + 1, \quad b \equiv \exp\left(\frac{\tilde{\zeta}}{2}\right) - 1, \quad \tilde{\phi} \equiv \frac{ze\phi}{kT} \tag{18}$$

and $\tilde{\zeta}$ is the nondimensional potential $\tilde{\phi}$ evaluated at the shear plane (i.e., the nondimensional ζ-potential). In the Debye−Hückel limit, this solution reduces simply to

$$\phi' = \frac{\zeta}{E^* d}\exp[-(y - y_w)/\lambda_D] \tag{19}$$

As pointed out by Hunter,[20] the Debye−Hückel approximation holds remarkably well for values of the nondimensional potential $\tilde{\phi}$ of approximately 2 or less.

Momentum Equation in the Inner Flow Region. An order of magnitude analysis is here used to investigate the effect of the forces within the thin electrical double layer on the equations of motion. We assume that the cases of interest are for a nondimensional electroosmotic flow velocity, u', of order one and for nondimensional time scales, t', of order one. We will also assume that, in all cases of interest, the characteristic length in the flow direction L is larger than d, so that λ_D/d and λ_D/L are both smaller than 10^{-4}. We define a smallness parameter δ' equal to λ_D/d.

For the cases of interest here, we consider the nondimensional streamwise coordinate x' as order one, and the transverse coordinate y' is taken as order λ_D/d. From the continuity eq 2, the order of the v' velocity in the electrical double layer must then be λ_D/d and therefore negligible. In our coordinate system, the x-component of momentum eq 3 is

$$StRe\frac{\partial u'}{\partial t'} + Re\left(u'\frac{\partial u'}{\partial x'} + v'\frac{\partial u'}{\partial y'}\right) = -\frac{\partial p'}{\partial x'} + \left(\frac{Re\epsilon E^{*2}}{\rho U^2}\right)\rho_E' E_x' + \left(\frac{\partial^2 u'}{\partial x'^2} + \frac{\partial^2 u'}{\partial y'^2}\right) \tag{20}$$

where the subscript on the electric field indicates an x-component. An order of magnitude analysis yields,

$$StReO(1) + Re\left(O(1)\frac{O(1)}{O(1)} + O(\delta')\frac{O(1)}{O(\delta')}\right) \sim -\frac{\partial p'}{\partial x'} + \left(\frac{Re\epsilon E^{*2}}{\rho U^2}\right)\rho_E' E_x' + \left(\frac{O(1)}{O(1)} + \frac{O(1)}{O(\delta'^2)}\right) \tag{21}$$

The operator $O(\pi)$ indicates the order of a quantity π. It is useful to approximate the order of the various terms above within the inner region of the flow for typical applications. The electrical body force term drives the flow and we must assume it is important. As mentioned above, for typical electroosmotic flow systems, the velocity scale U is less than about 10 mm/s, so that Re based on a 100-μm hydraulic diameter is of order unity or less. Therefore, within the inner region of the electrical double layer, the viscous stresses associated with transverse gradients of streamwise velocity clearly dominate streamwise gradients of streamwise velocity as well as the terms associated with the advection of momentum. Applying eq 7, the momentum equation then reduces to

$$StRe\frac{\partial u'}{\partial t'} + \frac{\partial p'}{\partial x'} = -Re\left(\frac{\epsilon E^{*2}}{\rho U^2}\right)\frac{\partial^2 \phi'}{\partial y'^2}E'_x + \frac{\partial^2 u'}{\partial y'^2} \tag{22}$$

Equation 22 is valid for the inner region of the flow and for typical electrokinetic flows with a Reynolds number of 10 or less. The inner region of the flow can be interpreted as being too thin to support the advection of momentum and viscous stresses associated with x-gradients of streamwise velocity. We can bound the region where the nonlinear term on the right-hand side of the equation is important by considering the decay of the electrical potential. The value of y for which the Lorentz body force is on

(20) Hunter, R. J. *Zeta Potential in Colloid Science*; Academic Press: London, 1981.

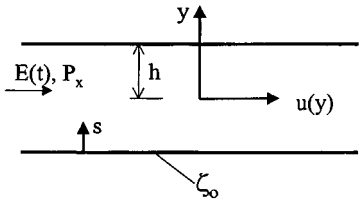

Figure 2. Schematic of a two-dimensional channel subjected to a constant pressure-gradient P_x and a step function in electric field $E(t)$. The top and bottom walls of the channels have a ζ-potential equal to ζ_o and the fluid flow in the channel is assumed to be fully developed.

the order of the viscous stresses can be determined by considering the relative magnitdue of the two terms in eq 22. Taking the nondimensional field as order unity, the condition at which the Lorentz body force is on the same order as the viscous force can be written as

$$\lambda_D^2\left(\frac{2Fz_i c_\infty E^*}{\eta U}\right)\sinh\left(\frac{ze\phi}{kT}\right) = O(1) \tag{23}$$

where we have used eq 14 to formulate the nondimensional potential term. This quantity can be interpreted as a local nondimensional ratio of Lorentz to viscous forces. In approximating the region where the Lorentz force disappears, we may accurately apply the Debye−Hückel limit since the local potential is low. Applying the Debye−Hückel limit of small wall potential, this condition reduces to

$$(\epsilon E^*/\eta U)\phi = O(1) \tag{24}$$

As will be shown below, in all flows with thin electrical double layers, the velocity magnitude at the top of the double layer is well approximated by $U = \epsilon E\zeta/\eta$, so that the condition expressed by eq 24 simply becomes $\phi/\zeta = O(1)$. Applying eq 19, the region where the Lorentz body force is on the order of the viscous force extends only a few Debye lengths from the wall (ϕ/ζ is less than 2% a distance of four Debye lengths from the wall). We will consider this the extent of the inner flow region. In the next two sections, we will analyze the accuracy of applying a slip approximation at the surface separating the inner and outer flow regions.

Pressure and Inertial Effects on Inner Flow. As described above, the only forces of importance in typical electroomostic flow systems are flow inertia, viscous stresses, pressure forces, and the Lorentz body force acting on the charges of the thin electric double layer. To investigate the effects of pressure and flow inertia on the inner flow region of the electrical double layer, we will consider an unsteady flow in the two-dimensional flow channel depicted in Figure 2. The channel is assumed to have a large width, a height h, and a uniform (and constant) wall zeta potential ζ_o. Before time $t = 0$, a fully developed flow has been established by a uniform pressure gradient P_x in the absence of an electric field. At time $t = 0$, an electric field E_o is applied in addition to the pressure gradient. As for typical microchannel applications, the relatively thin double layers at the walls of the channel can be treated as independent since $h \gg \lambda_D$, and the potential at $y = 0$ is zero. The flow field is well described by eq 22 which, in dimensional form, simplifies to

$$\frac{\rho}{\eta}\frac{\partial u(y,t)}{\partial t} + \frac{P_x}{\eta} = -\frac{\epsilon E_o}{\eta}\frac{d^2\phi(y)}{dy^2} + \frac{\partial^2 u(y,t)}{\partial y^2} \tag{25}$$

subject to initial and boundary conditions,

$$u(y,t=0) = -\frac{h^2 P_x}{2\eta}\left(1 - \frac{y^2}{h^2}\right) \tag{26a}$$

$$u(\pm h,t) = 0 \tag{26b}$$

$$\phi(\pm h,t) = \zeta_o \tag{26c}$$

The solution to eqs 25−26 can be obtained by a linear superposition of the unsteady flow solution given by Soderman and Jonsson[7] to the velocity field associated with a pressure-driven flow in the channel. The validity of this superposition can be shown by defining a new variable $F(y,t)$ defined as

$$F(y,t) \equiv u(y,t) + \frac{\epsilon E_o}{\eta}[\zeta_o - \phi(y)] \tag{27}$$

The equation of motion becomes

$$\frac{1}{\nu}\frac{\partial F(y,t)}{\partial t} = \frac{\partial^2 F(y,t)}{\partial y^2} - \frac{P_x}{\eta} \tag{28}$$

where ν is the kinematic viscosity of the fluid and the equation is subject to the following initial and boundary conditions:

$$F(y,t=0) = -\frac{h^2 P_x}{2\eta}\left(1 - \frac{y^2}{h^2}\right) + \frac{\epsilon E_o}{\eta}[\zeta_o - \phi(y)] \tag{29a}$$

$$F(\pm h,t) = 0 \tag{29b}$$

Equation 28 is linear, and the solutions for the cases where $P_x = 0$ and $E_o = 0$ can be linearly superposed. The solution for the case where $E_o = 0$ is simply

$$F(y;E_o = 0) = -\frac{h^2 P_x}{2\eta}\left(1 - \frac{y^2}{h^2}\right) \tag{30}$$

The solution for $F(y,t)$ for the case where $P_x = 0$ has been shown by Soderman and Jonsson[7] to be

$$F(y,t;P_x = 0) = \frac{\epsilon E_o \zeta_o}{\eta}[f(y,t)] \tag{31}$$

where

$$f(y,t) \equiv \sum_{n=0}^{\infty}\left\{2(-1)^n\left(\frac{1}{(n+0.5)\pi} - \frac{h\lambda_D}{h^2 + ((n+0.5)\pi\lambda_D)^2}\right)\cos\left(\frac{(n+0.5)\pi y}{h}\right)\exp\left(\frac{-(n+0.5)^2\pi^2\nu t}{h^2}\right)\right\} \tag{32}$$

Superposing these solutions, solving for the velocity $u(y,t)$ and rearranging

$$u(y,t) = -\frac{\epsilon E_o \zeta_o}{\eta}(1 - \theta(y,t)) \quad (33)$$

where

$$\theta(y,t) = \left[\frac{\phi(y)}{\zeta_o}\right] + [f(y,t)] + \left[-\frac{h^2 P_x}{2\epsilon E_o \zeta_o}\left(1 - \frac{y^2}{h^2}\right)\right] \quad (34)$$

The solutions for ϕ described earlier can now be used to estimate the effects of pressure and inertial forces throughout the velocity field for the case of thin (nonoverlapping) electrical double layers on the top and bottom walls. Together, all three terms in eq 34 bound the region where a slip surface approximation given by

$$u(y,t) = -(\epsilon E_o \zeta_o / \eta) \quad (35)$$

is accurate. The relation for θ above has been written so that the first, second, and third terms in brackets describe the effects of viscous stresses, flow inertia, and pressure, respectively, on the applicability of eq 35. The linear superposition of these three effects is a direct result of the linearity of eq 28. Note that θ is dependent on fluid viscosity only through inertial effects. Unlike the first two terms, the third term increases in magnitude as the distance s from the wall increases and scales as $2s/h - s^2/h^2$ (for $s < h$, see Figure 2).

Figure 3 shows a plot of the nondimensional velocity field predicted by eq 33. Example values of $h/\lambda_D = 3300$; $(h^2P_x)/(\epsilon E_o\zeta_o) = \pm 40$; and $4\nu t/\lambda_D^2 = 100$, 2500, and 62 500 were used to generate the plot. Figure 3a shows the velocity field near the wall in terms of the wall coordinate s shortly after the activation of the electric field for a channel subject to an adverse pressure gradient. Figure 3b shows velocity profiles for a favorable pressure gradient. Near the wall (e.g., for s less than about $2\lambda_D$ in the conditions shown in the figure), the velocity distribution is determined solely by the effects of viscous and electrostatic forces and all of the velocity profiles collapse to a single line. For s less than about 4 λ_D and long times after the application of the electric field, the terms on the left-hand side of eq 25 are neglible, and $\theta \cong \phi(y)/\zeta_o$ in this region. As time progresses, the velocity near approximately $s/\lambda_D = 4$ approaches that predicted by the Helmholtz−Smoulochowski equation (a nondimensional velocity of unity in the figure). As the distance from the wall increases, the inertial and pressure force terms in eq 25 become important and so the velocity field becomes dependent on time and the pressure gradient. For the thin-double-layer, two-dimensional microchannel considered here, eq 35 predicts the local velocity to within 2% for times greater than $10^5\lambda_D^2/\nu$, adverse pressure gradients (i.e., pressure gradients with the same sign as the electric field) with a magnitude less than $30\epsilon E_o\zeta_o/h^2$, and a distance from the wall equal to $4\lambda_D$. The effects of favorable pressure gradients and inertial forces due to an electric field directed along the x-direction partially offset each other so that, in such flows, the slip approximation becomes accurate for times less than $10^5\lambda_D^2/\nu$ (see Figure 3b).

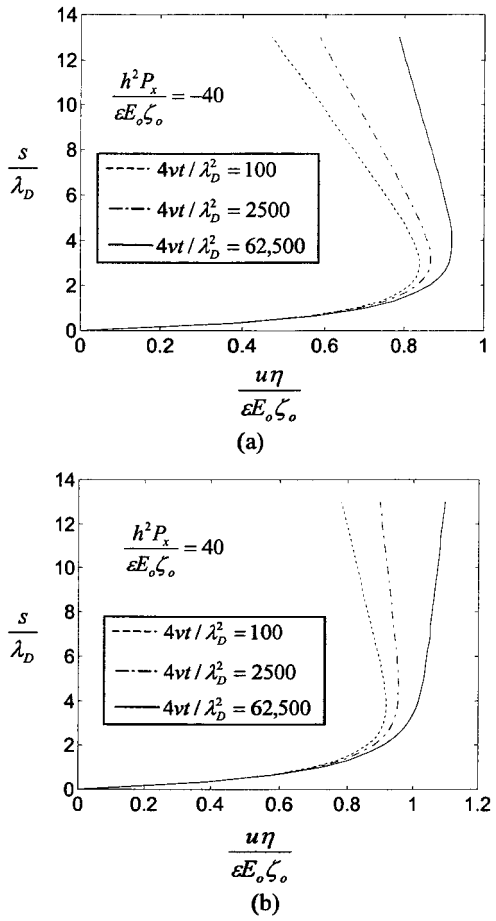

Figure 3. Nondimensional velocity profile within the two-dimensional channel shown in Figure 2 as a function of the nondimensional wall coordinate s/λ_D. Typical electrokinetic microchannel system values of $\zeta = -4$ and $h/\lambda_D = 3300$ were used to generate these velocity profiles.

The slip velocity approximation is clearly applicable for typical electroosmotic flow applications across a wide range of conditions, and in calculating the development of the outer flow solution, the slip velocity can be approximated as occurring at the wall. The electroosmotic flow example plotted in Figure 3 is consistent with a quasi-two-dimensional microchannel with $h = 10\ \mu$m, $\zeta = -100$ mV, and $\lambda_D = 3$ nm. The "long" time criteria of the inertial problem and the large distance from the wall requirement of the viscous problem for this example are on the order of 10^{-6} s and 12 nm, respectively, for θ less than 2%. If such a channel is driven by a value of 500 V/cm field, an adverse pressure gradient of approximately 100 kPa/cm is required before pressure effects increase the value θ to 2% for distances *less than* $4\lambda_D$ from the wall. Although such a pressure gradient is readily achievable in electrokinetic flow systems,[21−23] it is much larger than, for example, the inadvertent pressure gradients associated with differences in the hydrostatic pressure at electrokinetic channel reservoirs in microfluidic systems.

(21) Paul, P. H.; Arnold, D. W.; Rakestraw, D. J. Micro Total Analysis Systems Conference, Banff, Canada 1998.

(22) Zeng, S.; Chen, C.-H.; Mikkelsen, J. C., Jr.; Santiago, J. G. *Sens. Actuators B*, in press.

(23) Chen, C. H.; Zeng, S.; Mikkelsen, J. C., Jr.; Santiago, J. G. Development of a Planar Electrokinetic Pump. 2000 International Mechanical Engineering Congress and Exposition, Orlando, FL, November 5−10, 2000.

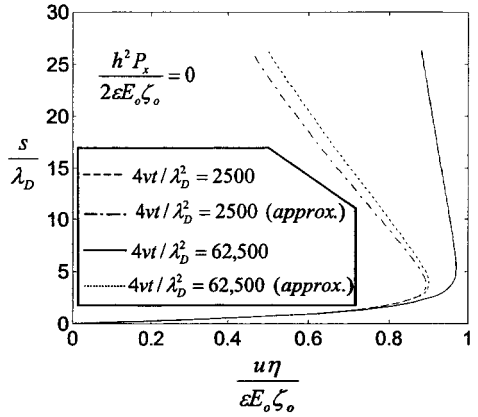

Figure 4. Comparison between the analytical velocity field prediction for electroosmotic flow in a two-dimensional microchannel and the approximation given by eq 37. Again, typical electrokinetic microchannel system values of $\tilde{\zeta} = -4$ and $h/\lambda_D = 3300$ were used to generate these profiles. For times greater than $10^3\lambda_D^2/\nu$ but less than $0.1h^2/\nu$, the velocity field is well approximated by eq 37.

Simplifying assumptions can be made in applying eq 33 to estimate the velocity field of the inner flow solution. The time for the inner flow solution to reach steady state is much smaller than time for the propagation of the momentum wave generated by the electric field to reach middle of the channel ($y = 0$). The inner-to-outer flow relaxation time ratio scales as λ_D^2/h^2, which is typically of order 10^{-8}. The second term in eq 34 can therefore be described by an approximate solution for the start-up flow of electroosmotic flow over a flat plate[7] and θ, near the bottom wall, can be approximated as

$$\theta(y,t) \cong \frac{\phi(y)}{\zeta_o} + \left[\left(1 - \frac{\phi(y+h)}{\zeta_o}\right)\mathrm{erf}\left(\frac{y+h}{\sqrt{4\nu t}}\right)\right] + \left[-\frac{h^2 P_x}{2\epsilon E_o \zeta_o}\left(1 - \frac{y^2}{h^2}\right)\right] \quad (36)$$

which is valid for short times such that $h \gg (4\nu t)^{0.5}$ and for the $y < 0$ portion of the channel. Further, in estimating the properties of the transition between inner and outer flow solutions, the Debye−Hückel approximation offers a very accurate approximation of ϕ so that we can write,

$$\theta(y,t) \cong \exp\left(-\frac{y+h}{\lambda_D}\right) + \left[\left(1 - \exp\left(-\frac{y+h}{\lambda_D}\right)\right)\mathrm{erf}\left(\frac{y+h}{\sqrt{4\nu t}}\right)\right] + \left[\frac{h^2 P_x}{2\epsilon E_o \zeta_o}\left(1 - \frac{y^2}{h^2}\right)\right] \quad (37)$$

The velocity profile is plotted in Figure 4 with a θ predicted by both eqs 34 and 37. The approximate near-wall velocity profile obtained using eq 37 and the profile predicted using eq 34 are very similar. For the later of the two times plotted, the difference between the two relations is indistinguishable in the plot. The approximate solution does very well in predicting the velocity field for times greater than $10^3\lambda_D^2/\nu$ and less than $0.1\ h^2/\nu$, where the upper bound is approximately the time when the inertial boundary layers from the top and bottom walls begin to interact. For the transition region between the inner and outer flows, where y is on the order of a few Debye lengths, eq 37 shows that the order of θ for long times is

$$\theta(y,t) \cong O[\lambda_D h P_x/\epsilon E_o \zeta_o] \quad (38)$$

The value of θ is clearly dominated by the pressure term throughout the outer flow in the steady-state solution.

Last, consider the velocity gradient at the boundary between the inner and outer flow regions. From eq 33,

$$\frac{\partial u(y,t)}{\partial y} = \left[\frac{\epsilon E_o}{\eta}\frac{\mathrm{d}\phi(y)}{\mathrm{d}y}\right] + \left[\frac{\epsilon E_o \zeta_o}{\eta}\frac{\partial f(y,t)}{\partial y}\right] + \frac{P_x y}{\eta} \quad (39)$$

Equation 39 describes the shear rate of the fluid in terms of the viscous, inertial forces, and pressure forces throughout the channel. The first bracketed term decays within a few Debye lengths from the wall. At the boundary between the inner and outer flow regions, the velocity gradient is therefore well approximated by the terms involving the pressure gradient and the inertial forces in the channel. Note that these terms result in a nonzero velocity gradient at the slip plane. The velocity field at the slip surface can therefore be approximated as a slip velocity condition that can support the velocity gradients associated with pressure and inertial forces. This ability for the "slip plane" in Figure 1 to sustain both a slip velocity and a shear stress makes it very different from the slip velocity models often applied in irrotational flow theory.

Quasi-Steady Slip Condition. As we have seen, the equations of motion are linearized within the electrical double layer despite the characteristics of the bulk flow outside of it. This linearization and the associated simplicity of the equations allow us to, for the general cases of arbitrary *Re* and *St* outside the electrical double layer, approximate the velocity at the slip plane by that predicted for a simple case of a flat wall with zero pressure gradient and negligible intertial effects. For the case of unsteady flows at typical conditions and with finite *Re*, finite *ReSt*, and pressure gradients significantly lower than $30\epsilon E_o \zeta_o/h^2$, the velocity at the local slip plane can be well approximated by the simple electroosmotic relation for noninertial electroosmotic flow in a plane wall

$$\bar{u}_{\mathrm{slip}} = -\left(\frac{\epsilon\bar{\zeta}\bar{E}}{\eta}\right) = \mu\bar{E} \quad (40)$$

Here $\bar{u}$ and $\bar{E}$ are local functions of time. μ is a characteristic mobility parameter defined by eq 40. In the physical case, ϵ and η vary within the electrical double layer. Indeed, in electrical double layers in general, noncontinuum effects such as finite-ion size effects and gradients in the dielectric strength and viscosity of the fluid are important as described in detail by Hunter.[20] Because of this complexity, the ζ-potential in eq 40 can, in practice, be interpreted as an empirically measured mobility parameter that determines the local velocity of the bulk flow at the top of the electrical double layer. The ζ-potential can be only approximately related to the local surface charge density on the wall and the bulk fluid properties by applying a continuum assumption.

To summarize the analysis above, we can state that the justification for eq 40 is that, within the inner flow region of thin-

double-layer electroosmotic flows, the electrostatic body force is balanced primarily by the viscous drag force and all other terms in the equation of motion are negligible. The solutions for the velocity fields of bulk flow and of the flow within the electrical double layer are therefore uncoupled. This simplification is more complete than the classical uncoupling between boundary layer and free streamflow fields in classical macroscale systems since, in the electroosmotic flow case, there is no need to couple the pressure field solution between the inner and outer flows.

We can approximate conditions required for the applicability of the slip velocity model in typical electroosmotic flows in microchannels with a hydraulic diameter d. The approximate conditions are as follows: electric double-layers thin compared to channel dimension: $d/\lambda_D > 10^3$; times longer than $10^5\lambda_D^2/\nu$ after rapid changes in electric field; distances y from the wall equal to approximately $4\lambda_D$; Reynolds number based on d less than 10; pressure gradient magnitudes lower than $30\epsilon E_o\zeta_o/\boldsymbol{h}^2$.

The values chosen here make outer flow velocities made using the slip surface model accurate to within about 2% in the two-dimensional channel which was analyzed here.

U AND *E* SIMILARITY FOR UNIFORM **Z**-POTENTIAL IN OUTER FLOW

For simple conditions, the electroosmotic flow in the outer flow region is simply equal to the local electric field multiplied by a constant. This section presents a brief analytical development of this concept in electroosmotic flows for the case of uniform, constant wall ζ-potential. We again formulate the problem for the outer flow solution using eqs 1−7. For the general case of unsteady electroosmotic flow with finite inertial effects and through an arbitrary geometry, the electric field can be expressed as

$$\nabla' \cdot \bar{E}' = 0 \tag{41}$$

and

$$\nabla' \times \bar{E}' = 0 \tag{42}$$

since the charge density in the outer flow solution is zero. We are interested in finding solutions to eqs 2 and 3 which, for the outer flow, reduce to

$$\nabla \cdot \bar{V}' = 0 \tag{43}$$

$$StRe\,\frac{\partial \bar{V}'}{\partial t'} + Re\bar{V}' \cdot \nabla' \bar{V}' = -\nabla' p' + (\nabla'^2 \bar{V}') \tag{44}$$

subject to the slip velocity and inlet/outlet boundary conditions

$$\bar{V}' = \mu_o' \bar{E}' \quad \text{(at slip surface)} \tag{45}$$

$$\bar{V}' = \mu_o' \bar{E}' \quad \text{(at inlets and outlets)} \tag{46}$$

where μ_o' is a constant, uniform value of the mobility at the wall. Equation 46 assumes that the inlet and outlet flows are irrotational so that we are considering the case where there are zero pressure gradients at the inlets and outlets.

As mentioned earlier, Overbeek[12] proposed that electroosmotic flow outside of very thin electrical double layers in fluid channels of arbitrary geometry is irrotational for the case of low Reynolds number and zero pressure gradients. Because Overbeek considered the linear, steady Stokes equations of motion bounded by a slip surface, for his case, the irrotational solution is unique. His approach was to hypothesize an irrotational solution and show that it is a solution to the equations of motion with zero applied pressure gradient. A similar approach is used here to examine a set of conditions that lead to irrotational outer flow velocity fields. First, we hypothesize a solution of the form

$$\bar{V}' = c_o \bar{E}' \quad \text{(throughout the field)} \tag{47}$$

Here c_o is an undetermined constant and $\bar{V}'$ and $\bar{E}'$ are the local values of velocity and electric field throughout the domain. We then ask what conditions must be met in order for eq 47 to be a solution to eqs 43 and 44, given eqs 41 and 42.

First, from the condition expressed by eq 41, we know that eq 43 is satisfied by eq 47. Next, we use an identity for the Laplacian of a vector to expand the viscous term in eq 44 and substitute eq 47

$$\nabla^2 \bar{V}' = \nabla'(\nabla' \cdot \bar{V}') - \nabla' \times \nabla' \times \bar{V}' = c_o \nabla'(\nabla' \cdot \bar{E}') - c_o \nabla' \times \nabla' \times \bar{E}' \tag{48}$$

The first term on the right-hand side of eq 48 is zero by eq 41. From the irrotationality condition of the electric field, we know the last term on the right-hand side of eq 48 is also zero. Therefore, as expected, the viscous term for solutions of the form given by eq 47 is identically zero and eq 44 then reduces to

$$StRe\,\frac{\partial \bar{V}'}{\partial t'} + Re\bar{V}' \cdot \nabla' \bar{V}' = -\nabla' p' \tag{49}$$

Equation 49 is not a new governing equation but rather a necessary condition for eq 47 to be a solution to the equations of motion. We find that this relation holds for at least one case applicable to electrokinetic microfluidics applications. Namely, if we consider flows with both a very low Reynolds number and a low *ReSt* product, the inertial terms on the left-hand side of eq 44 are negligible. For such flows, common to on-chip electroosmotic flow applications, the condition for eq 47 to hold reduces to

$$\nabla' p' \cong 0 \tag{50}$$

Hence, electroomostic flows with uniform pressure, low *Re*, and low *ReSt* have a velocity field similar to the electric field. This pressure gradient condition applies to both externally applied and internally generated pressures. However, the internally generated pressures in low *Re* and low *ReSt* electroosmotic flows with zero net pressure drop between inlets and outlets are typically only found in flows in microchannels with nonuniform ζ-potentials,[4] which we have not considered here since such flows are clearly rotational.

The range of applicability of the irrotational solution to flows with finite *Re* and *ReSt* is unproven and difficult to generalize because of the nonlinearity of the full Navier−Stokes formulation.

There may perhaps be other flow fields for which the condition expressed by eq 49 holds without the disappearance of the terms on the left-hand side of eq 44. However, such flows are probably not found in microfluidics applications. For example, one type of flow for which eq 49 provides accurate results are very high Reynolds number freestream flows (e.g., flow external to a boundary layer region around a streamlined body) where the inertial and pressure force terms in the equation of motion are much larger than the viscous terms. This aerodynamics approximation is often applied in incompressible, high-Reynolds number flows,[24] but is of little importance to electroosmotic flows. Another example that is common to electrokinetics applications is the case of low Reynolds number where the condition for similarity reduces to

$$StRe(\partial \bar{V}'/\partial t') \cong -\nabla' p' \tag{51}$$

However, it is unlikely that this condition would hold throughout an electroosmotic flow field. As discussed earlier, the flow relaxation times associated with changes in the inner flow region are much shorter than the relaxation times associated with the outer flow. The typical outer-to-inner flow relaxation time ratio is 10^8 so that it is unlikely that any thin-double-layer transient electroosmotic outer flow of interest can satisfy both eqs 47 and 51 and the boundary conditions eqs 45 and 46 at all times.

Last, we can evaluate the hypothesized constant c_o in the proposed solution by applying the boundary conditions (eqs 45 and 46) to find that

$$c_o = \mu_o' \tag{52}$$

so that the Helmholtz−Smoulochowski equation that holds for thin-double-layer electroosmotic flows also holds for the velocity field of electroosmotic flows in uniform ζ-potential systems or, in dimensional form

$$\bar{V} = -(\epsilon \zeta \bar{E}/\mu) \tag{53}$$

where $\bar{E}$ is the local electric field, $\bar{V}$ is the velocity of the fluid throughout the field, and ζ is the ζ-potential at the wall.

We can summarize the set of sufficient (but not necessarily unique) conditions for which there exist an outer flow velocity field solution that is similar to the electric field as follows: electric double layers thin compared to channel dimension; uniform ζ-potential; uniform fluid properties; electrically insulating channel walls; low Reynolds number; low product of Reynolds and Strouhal numbers; parallel flow at inlets and outlets; equal pressure at all inlets and outlets.

An experimental visualization of the similarity between the electric and velocity fields of an electroosmotic flow[25] is presented in Figure 5. The figure shows a comparison between imaged electrokinetic particle path lines at a microchannel intersection and predicted electric field lines (shown as white lines superposed on the image). The path line visualization was obtained using 0.5-μm-diameter fluorescent polystyrene particles flowing through an intersection of two microchannels. The microchannels (courtesy of Aclara Biosciences, Mountain View, CA) are fabricated in acrylic using an embossing method and have a roughly trapezoidal cross section that is 130 μm wide at the top, 60 μm wide at the base, and 50 μm deep. The electrophoretic mobilities of the particles and the electroosmotic flow mobility of the channel walls are approximately equal in magnitude so that deviations between the fluid velocity field and electric field should be readily apparent. The electric field line prediction was obtained using CFD Research Corporation's ACE code (Huntsville, AL). The predicted electric field lines very closely approximate the experimentally determined path lines of the flow. A similar visualization is presented by Cummings et al.[14] for steady electroosmotic flow in a sudden contraction.

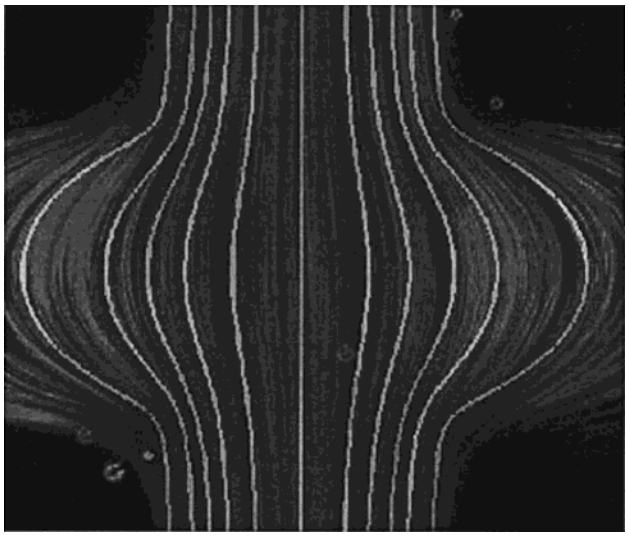

Figure 5. Comparison between electrokinetic flow path lines and predicted electric field lines in a steady, low Reynolds number flow in a system with uniform ζ-potential.[24] The flow field was imaged in the region of intersection of two acrylic microchannels with a trapezoidal cross section (130 μm wide at the top, 60 μm wide at the base, and 50 μm deep). The path lines in near a plane 10 μm from the top (wide) wall of the channel were imaged with a 60× oil immersion lens with a depth of field of approximately 2 μm. The flow tracers are polysterene microspheres 0.5 μm in diameter with an electrokinetic mobility approximately equal in magnitude to the electroosmotic flow mobility of the microchannel system.

Last, the current analysis suggests that flows with finite *Re* and finite *ReSt* products, in general, imply a violation of the similarity between the electric and velocity fields. The *Re* dependence suggested by the present analysis agrees with the results of the numerical modeling efforts of Patankar and Hu for electroosmotic flow with a finite *Re*.[7] In comparison, Cummings et al.[14] concluded that the irrotational solution should hold when inertial effects are not neglible. The reason for this discrepancy may be that Cummings et al. assumed that the irrotational solution for the Navier−Stokes equations of motion in electroosmotic flows is a stable and unique solution regardless of Reynolds number. Solutions to the fully nonlinear Navier−Stokes equations are not generally unique. Although the irrotational flow solution certainly applies to the outer flow for all Reynolds numbers (with a boundary of the flow taken as the slip surface as presented here), the solution may not be stable and may not model the actual flow

(24) Batchelor, G. K. *An Introduction to Fluid Dynamics*; Cambridge University Press: Cambridge, U.K., 1994.

(25) Devasenathipathy, S.; Santiago, J. G. Unpublished results, Stanford University, Stanford, CA, 2000.

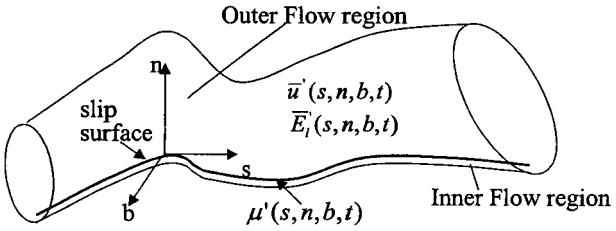

Figure 6. Electroosmotic flow in a microchannel of arbitrary geometry with nonuniform, unsteady wall mobility. The slip surface near the bottom of the channel is depicted in the figure and assumed to be very close to the wall.

at high *Re*. Note that the contention that the irrotationality condition holds regardless of all inertial effects is clearly not true for unsteady flows with finite *ReSt* as, for example, demonstrated by the two-dimensional channel solution presented earlier (when evaluated for $P_x = 0$). A formulation of the generation of vorticity at the slip surface due to finite *Re* and *ReSt* effects also suggests that this similarity may not hold for finite values of *Re*. This formulation is presented below.

VORTICITY PRODUCTION IN OUTER FLOW SOLUTION

The outer flow velocity field is depicted in Figure 6 for an arbitrarily shaped electroosmotic microchannel bounded by a slip surface boundary with an arbitrary (time-dependent) wall mobility distribution. Following the analysis of the previous sections, we assume that the velocity of the slip plane is described by eq 53 and that, at the slip plane, the velocity gradients are determined by the properties of the outer flow conditions and the local values of wall ζ-potential. For the case of a "smooth" microchannel with radii of curvature much larger than the Debye length of the electrolyte, we can define a locally orthogonal streamline coordinate system for the outer flow. The unit normals of this streamline coordinate system are $\hat{s}$, $\hat{n}$, and $\hat{b}$, and the velocity components are u_s, u_n, and u_b in the *s* (streamwise), *n* (normal), and *b* (binormal) directions, respectively. The coordinates *s*, *n*, and *b* are again nondimensionalized using the hydraulic diameter of the channels. The electroosmotic mobility μ is equal to $\epsilon\zeta/\eta$ and is nondimensionalized by E^*/U.

In the bulk, the net charge density in the fluid is identically zero and Gauss's law describing the electric field lines reduces to

$$\nabla' \cdot \bar{E}_l' = 0 \tag{54}$$

where $\bar{E}_l'$ is the electric field in the streamline coordinate system. Since the effects of induced electric fields due to changing magnetic fields in these systems is typically negligible, Faraday's law of induction reduces to

$$\nabla' \times \bar{E}_l' = 0 \tag{55}$$

where, again, the curl operator has been nondimensionalized with the characteristic hydraulic diameter of the channel, *d*. The continuity relation (eq 2) has the same form but the equations of motion are now coupled to the electric field only through the boundary condition at the slip surface and can be written as as

$$St\frac{\partial \bar{u}'}{\partial t'} + \bar{u}' \cdot \nabla' \bar{u}' = -\frac{1}{Re}\nabla p' + \frac{1}{Re}(\nabla'^2 \bar{u}') \tag{56}$$

The insulated and impenetrable wall boundary conditions are

$$\bar{E}_l' \cdot \hat{n} = 0 \qquad \text{at the slip plane} \tag{57}$$

$$\bar{u}_l' \cdot \hat{n} = 0 \qquad \text{at the slip plane} \tag{58}$$

We shall make the very accurate assumption that the wall normal is identical to that of the slip plane throughout the domain of interest (i.e., a thin electrical double layer). The velocity at the wall is then expressed as

$$\bar{u}' = \mu'(s,n,b,t)\bar{E}_l' \qquad \text{at the slip plane} \tag{59}$$

where the nondimensional mobility μ' describes the relationship between the slip surface velocity and the electric field and is a scalar field defined on the slip surface. Note that rapidly varying wall mobilities are of interest and, for example, applicable to efforts that aim to control electroosmotic flow using externally applied fields.[21] Equation 59 assumes that the electrical double-layer mobility is isotropic in the slip plane surface.

We will express the dynamics of the system in terms of the fluxes of vorticity at the boundaries of the flow in order to identify the effects that lead to a loss in similarity between the electric and velocity fields. Vorticity can be generated in electrokinetic microchannels at the slip planes of the channels where, as we have seen, there can exist a constraint on the second derivative of streamwise velocity in the equations of motion. In streamline coordinates, the nondivergence and irrotational criteria given by Gauss's and Faraday's laws, respectively, are

$$\frac{\partial E_s'}{\partial s'} + \frac{\partial E_n'}{\partial n'} + \frac{\partial E_b'}{\partial b'} = 0 \tag{60}$$

and

$$\left(\frac{\partial E_b'}{\partial n'} - \frac{\partial E_n'}{\partial b'}\right)\hat{s} + \left(\frac{\partial E_s'}{\partial b'} - \frac{\partial E_b'}{\partial s'}\right)\hat{n} + \left(\frac{\partial E_n'}{\partial s'} - \frac{\partial E_s'}{\partial n'}\right)\hat{b} = 0 \tag{61}$$

Here, the electric field in the streamline coordinate system is nondimensionalized by the characteristic field E^* and has components E_s, E_n, and E_b. In the streamline coordinate system, the continuity equation is

$$\frac{\partial u_s'}{\partial s'} + \frac{\partial u_n'}{\partial n'} + \frac{\partial u_b'}{\partial b'} = 0 \tag{62}$$

The three components of the momentum equation evaluated at

the slip surface are

$$St\frac{\partial u_s'}{\partial t'} + u_s'\frac{\partial u_s'}{\partial s'} = -\frac{1}{Re}\frac{\partial p'}{\partial s'} + \frac{1}{Re}\left(\frac{\partial^2 u_s'}{\partial s'^2} + \frac{\partial^2 u_s'}{\partial n'^2} + \frac{\partial^2 u_s'}{\partial b'^2}\right) \quad (63)$$

$$u_s'\frac{\partial u_n'}{\partial s'} = -\frac{1}{Re}\frac{\partial p'}{\partial n'} + \frac{1}{Re}\left(\frac{\partial^2 u_n'}{\partial s'^2} + \frac{\partial^2 u_n'}{\partial n'^2} + \frac{\partial^2 u_n'}{\partial b'^2}\right) \quad (64)$$

$$u_s'\frac{\partial u_b'}{\partial s'} = -\frac{1}{Re}\frac{\partial p'}{\partial b'} + \frac{1}{Re}\left(\frac{\partial^2 u_b'}{\partial s'^2} + \frac{\partial^2 u_b'}{\partial n'^2} + \frac{\partial^2 u_b'}{\partial b'^2}\right) \quad (65)$$

where streamline coordinate velocities are nondimensionalized by a characteristic velocity U and the Reynolds number is based on the channel diameter d. The pressure, p, is nondimensionalized by the viscous pressure $\eta U/d$. This pressure nondimensionalization is appropriate here because we are interested mostly in flows with Reynolds numbers of order unity or less.

First, we evaluate the relations for the electric field in the streamline coordinate system at the slip plane. We will denote the evaluation of a property at the slip plane with a subscript "sp" so that for any quantity π,

$$\pi_{sp} = \pi(s, 0, b, t) \quad (66)$$

From the condition that the transverse current into the electrical double layer is zero (eq 57):

$$E_{n,sp} = 0 \quad (67)$$

$$\frac{\partial E_n'}{\partial b'}|_{sp} = \frac{\partial E_n'}{\partial s'}|_{sp} = 0 \quad (68)$$

Evaluating the boundary condition (eq 59) at the slip plane and differentiating we find

$$u = \mu' E_{s,sp} \quad (69)$$

$$\frac{\partial u_n'}{\partial b'}|_{sp} = \frac{\partial u_n'}{\partial s'}|_{sp} = \frac{\partial u_b'}{\partial b'}|_{sp} = \frac{\partial u_b'}{\partial s'}|_{sp} = 0 \quad (70)$$

For the electric field,

$$E_{b,sp} = 0 \quad (71)$$

$$\frac{\partial E_b'}{\partial s'}|_{sp} = \frac{\partial E_b'}{\partial b'}|_{sp} = 0 \quad (72)$$

Note that, given the conditions described by eq 70, the vorticity vector at the slip plane is simply

$$\bar{\omega}' = \omega_s'\hat{s} + \omega_n'\hat{n} + \omega_b'\hat{b} = \frac{\partial u_b'}{\partial n'}\hat{s} + \frac{\partial u_s'}{\partial b'}\hat{n} - \frac{\partial u_s'}{\partial n'}\hat{b} \quad (73)$$

The vorticity is nondimensionalized using a characteristic time t^*. Evaluating eq 61 at the slip plane and applying the constraints on the electric field gradients at the slip plane (eqs 68 and 72),

$$\frac{\partial E_b'}{\partial n'}|_{sp} = \frac{\partial E_s'}{\partial b'}|_{sp} = \frac{\partial E_s'}{\partial n'}|_{sp} = 0 \quad (74)$$

In the streamline coordinate system, the only nonzero spatial gradients for electric field in the streamline coordinate system are $(\partial E'_s/\partial s')_{sp}$ and $(\partial E'_n/\partial n')_{sp}$. Evaluating the momentum relations given by eqs 63−65 at the slip plane and applying eqs 67−74,

$$\frac{\partial \omega_b'}{\partial n'} - \frac{\partial \omega_n'}{\partial b'} = ReSt\frac{\partial(\mu' E_s')}{\partial t'} + Re\mu' E_s'\frac{\partial(\mu' E_s')}{\partial s'} - \left(\frac{\partial^2(\mu' E_s')}{\partial s'^2}\right) + \frac{\partial p'}{\partial s'} \quad (75)$$

$$\frac{\partial \omega_b'}{\partial s'} - \frac{\partial \omega_s'}{\partial b'} = \frac{\partial p'}{\partial n'} \quad (76)$$

$$\frac{\partial \omega_s'}{\partial n'} - \frac{\partial p'}{\partial b'} \quad (77)$$

where the streamwise velocity component has been expressed using eq 59. Equations 75−77 demonstrate the relationship between the effects of unsteadiness, advection of momentum, gradients of wall mobility, and pressure gradients on the generation of vorticity at the slip plane of a thin electrical double-layer electroosmotic flow channel. We can use these equations to formulate the conservation of vorticity in arbitrarily shaped microchannels. Note that, for irrotational inlet and outlet flows, the fluxes of vorticity normal to the microchannel wall and into the outer flow are zero for the case of zero pressure gradients, zero gradients of wall mobility, and neglible values of Re and $ReSt$. Therefore, this formulation is consistent with the analysis regarding a set of sufficient conditions required for irrotational flow which was presented earlier.

These vorticity production relations show characteristics that are not found in equivalent expressions for viscous, no-slip flow fields.[26] In particular, the unsteady term in eq 75 includes the effect of temporal changes in wall charge and the advection of momentum term shows the effects of spatial gradients of wall mobilities. We also see that, despite the fact that the Re and St may be small and the electric field constant, large values of the products $St\partial\mu'/\partial t'$ and $Re\partial\mu'/\partial s'$ result in flow regimes where inertial effects are important, so that, despite conditions of low Re and St, flow fields with high temporal and spatial gradients in wall charge can show finite inertial effects. The temporal effect may be important in systems that aim to actively control charge layers by externally applied electric fields,[27] while the spatial effect would be relevant to efforts that aim to pattern (e.g., with microlithography) wall regions with materials of different surface charge density. Other terms in eqs 75−77 not found in the simple, viscous no-slip flows are the shear stresses and consequent generation of vorticity associated with gradients in wall mobility as well as the fact that,

(26) Panton, R. L. *Incompressible Flow*, 2nd ed.; John Wiley and Sons: New York, 1996.
(27) Schasfoort, R. B. M.; Schlautmann, S.; Hendrikse, L.; vandenBerg, A. *Science* **1999**, *286*, 942−945.

Table 1. Qualitative Interpretation of Parameters Describing the Production of Vorticity in the Electroosmotic Slip Surface

parameter	qualitative interpretation
Re	ratio of (advective component of) inertia to viscous forces
$ReSt$	ratio of local inertial forces to viscous forces (e.g., given an unsteady forcing function with a characteristic time t^*)
$Re\mu' E_s'^2 \partial(\mu')/\partial s'$	ratio of inertia associated with spatial mobility gradients to viscous forces
$StReE_s' \partial\mu'/\partial t'$	ratio of local inertial forces associated with temporal mobility changes to viscous forces
$Re\mu'^2 E_s' \partial(E_s')/\partial s$	ratio of inertia associated with gradients in electric field to viscous forces
$StRe\mu' \partial E_s'/\partial t'$	ratio of local inertial forces associated with temporal changes in electric field to viscous forces

unlike the no-slip case, the *n*-component of vorticity at the boundary is nonzero. Note also that some components of vorticity are diffused in the direction parallel to the slip plane so that these vorticity components seem to remain within the double layer. A qualitative physical interpretation of each of the important parameters describing the production of vorticity at the electroosmotic slip surface are given in Table 1. Equations 75−77 are applicable to the development of numerical efforts for simulating electroosmotic flows with finite inertia effects, wall-charge gradients, and pressure gradients. These equations are particularly useful for vorticity formulations[28] of electroosmotic flows.

EXAMPLE APPLICATIONS OF CURRENT ANALYSIS

As mentioned earlier, the development of electroosmotic microfluidic systems for bioanalytical analysis has spurred an interest in the design, visualization, and modeling of electroosmotic flow fields. This section presents two example applications of the current paper in the analysis of electrokinetic microchannel systems.

Measurement of Effects of Nonuniform ζ-Potentials in Electroosmotic Flows. Most ideal electrokinetic microchannel designs consist of uniform ζ-potential systems designed to operate in low *Re* and low *ReSt* conditions. However, actual systems can suffer from nonideal effects such as spatial gradients in ζ-potential due to variations in material properties and the chemical environment of surfaces. This effect clearly causes a breakdown of the similarity between the fluid velocity and electric field in the microchannel. This section presents a brief extension of the present analysis which suggests that effects of nonuniform wall charges can be measured directly by measuring the vorticity of flow tracers. The measured velocity field of a flow tracer (e.g., a fluorescent particle) of uniform mobility ν_t can be expressed as

$$\bar{u}_t = \bar{u} + \nu_t \bar{E} \tag{78}$$

Here $\bar{u}_t$ and $\bar{u}$ are the velocity fields of the tracer and the fluid, respectively. For uniform fluid properties (e.g., barring significant temperature gradients), the curl of eq 78 yields

$$\bar{\omega}_t = \bar{\omega} \tag{79}$$

where $\bar{\omega}_t$ and $\bar{\omega}$ are the vorticity of the electrophoretic tracer field and the fluid velocity field, respectively. Therefore, the measured vorticity field of the flow tracer is identical to the flow vorticity and the effects of nonideal wall charge distributions on vorticity production may be measurable directly using velocity field measurements. For example, referring to Figure 6, the flow in a straight microchannel with ζ-potential gradients in the *s*-direction will diffuse *b*-component vorticity in the direction normal to the wall. This component of vorticity can be measured from velocities in the $s-n$ plane. The resolution required for such measurements is within the capability of current particle-based velocity tracking methods.[29]

Development of Scalar Fields in Simple Electroosmotic Flows. Several groups have identified the challenges of calculating the effects of arbitrary electrosmotic channel geometries on the development of scalar fields.[30−32] Of particular interest is the development of electrophoretic analyte bands and sample streams as they travel through curved channels and intersections. The dispersive effects of microchannel geometries on scalars are often maximized in the case of flows with high advection-to-diffusion flux ratios (i.e., high Peclet number flows). As a consequence of the fluid velocity and electric field similarity described above, the development of electrophoretic bands in such flow fields reduces to a calculation of line integrals of the electric field. That is, the Lagrangian formulation for the location of any scalar quantity *s* along a time line can be expressed as

$$\frac{d\bar{s}(t)}{dt} = (\nu + \nu_t)\bar{E}(\bar{x},t) + \bar{\Psi}(\bar{x},t) \tag{80}$$

where ν is the uniform wall mobility of the electroosmotic flow and ν_t is the electrophoretic mobility of the scalar. $\bar{\Psi}(\bar{x},t)$ is a stochastic function that accounts for the effects of diffusion.[33] An approach similar to this has been applied by Molho et al.[31] to the design of finite Peclet number electroosmotic flow channel turns with minimal dispersion. The flow visualizations of Molho et al. are also an example of a simple electroosmotic flow with a velocity field similar to the electric field.

For the case of steady, high Peclet number flows (i.e., negligible mass diffusion), this relation reduces to simply

$$\frac{d\bar{s}(t)}{dt} = (\nu + \nu_t)\bar{E}(\bar{x}) \tag{81}$$

Equation 81 can be used to calculate the development of scalar quantities in electrokinetic flows from solutions of the electric field.

(28) Saffman, P. G. *Vortex Dynamics*; Cambridge University Press: Cambridge, U.K., 1995.

(29) Santiago, J. G.; Wereley, S. T.; Meinhart, C. D.; Beebee, D. J.; Adrian, R. J. *Exp. Fluids* **1998**, *25*, 316−319.

(30) Culbertson, C. T.; Jacobson, S. C.; Ramsey, J. M. *Anal. Chem.* **1998**, *70*, 3781−3789.

(31) Molho, J. I.; Herr, A. E.; Mosier, B. P.; Santiago, J. G.; Kenny, T. W.; Brennen, R. A.; Gordon, G. Micro Total Analysis Systems Conference, Enschede, The Netherlands, 2000.

(32) Legally, E. T.; Paegel, B. M.; Mathies, R. A. Micro Total Analysis Systems Conference, Enschede, The Netherlands, May 14−18 2000.

(33) Aref, H.; Naschie, M. S. E. *Chaos Applied to Fluid Mixing*; Pergamon Press: New York, 1995.

Equation 81 places certain constraints on the development of scalars in high-Peclet number electroosmotic flows. For example, these relations show that, for flows with high Peclet numbers, the similarity between the electric and velocity fields in simple flows requires that the angle between any time line (e.g., the loci of maximum concentration of an electrophoretic band) and the slip plane be constant for all time. This is a direct result of the irrotationality of the outer flow.

CONCLUSIONS

In electroosmotic flows within microfabricated channel networks, the charge double-layer thickness is typically small compared to both channel dimensions and the radii of curvature of channel geometries. For typical conditions, the velocity field in such flows can be separated into inner and outer flow regions. In the inner flow region, the fluid dynamics are dominated by the opposition of viscous and electrostatic forces and are uncoupled from the dynamics of the outer flow region. This uncoupling is therefore more complete than the classical uncoupling of boundary layer and freestream flow dynamics in macroscale flow applications as there is no need to match a pressure field solution. The outer flow region is clearly affected by pressure, inertia, and nonuniform surface charge. The two regions are separated by a slip surface which is locally well-approximated by the Helmholtz−Smoulochowski relation in typical microchannel applications. The vorticity production at this slip boundary can be modeled as a simple linear superposition of the slip velocity and the velocity field associated with the forces of pressure, inertia, and nonuniform mobilities. An analysis of the conditions required for similarity between the electric and velocity fields as well as the formulation of the vorticity production in such channels suggests that a certain set of conditions for similarity is met by many typical electroosmotic flow applications. For flow in a microchannel system with insulating walls with uniform surface charge, a sufficient set of conditions are low Reynolds number flow with a low Reynolds and Strouhal number product, zero applied pressure differences between all inlets and outlets, and uniform fluid properties. Finally, a few of the conclusions of the present study were discussed in the context of the measurement of surface charge gradients and the modeling of scalar field development in microfabricated electroosmotic systems.

ACKNOWLEDGMENT

This research was supported by the Defense Advanced Research Projects Agency contract F30602-00-2-0609 with Dr. A. Krishnan as monitor.

Received for review January 31, 2001. Accepted February 6, 2001.

AC0101398